Expanded View Figures

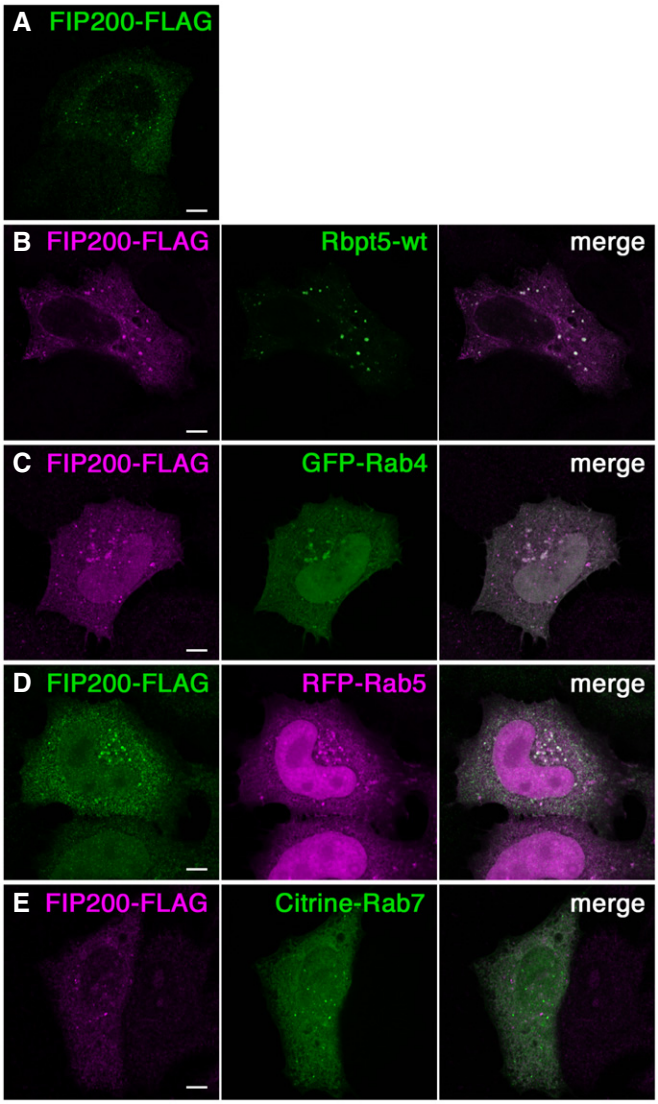

Figure EV1. FIP200 colocalizes with endosomal markers.

A–E HeLa cells were transfected with FLAG-tagged FIP200 alone (A) or together with Rabaptin5 (Rbpt5-wt) (B), GFP-Rab4 (C), RFP-Rab5 (D), or Citrine-Rab7 (E), fixed after 24 h, and subjected to immunofluorescence microscopy. Scale bar, 10 μm.

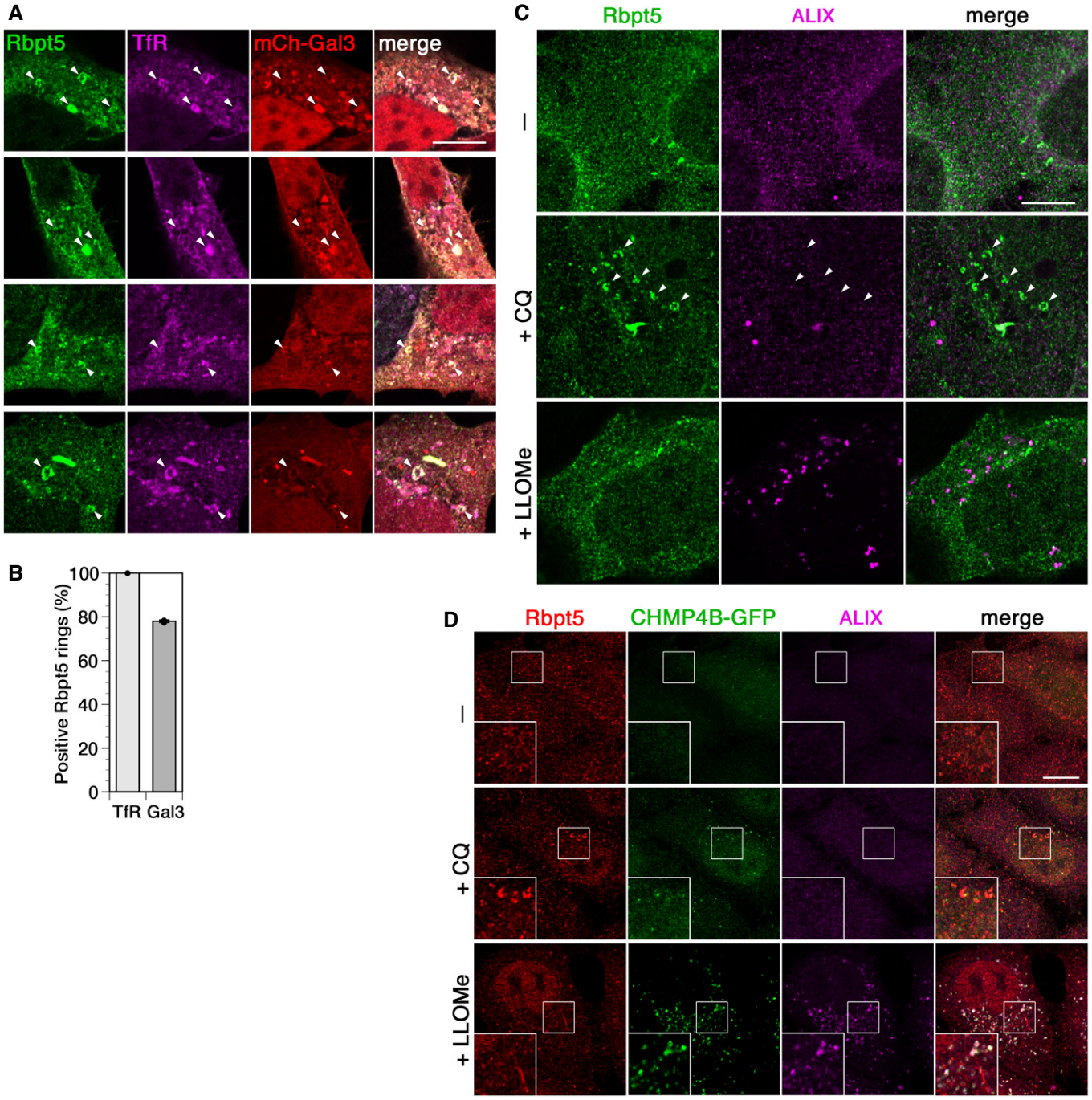

Figure EV2. Chloroquine damages transferrin receptor- and Galectin 3-positive early endosomes without recruiting ESCRT components.

A HEK^{+Rbpt5} cells transfected with mCherry-galectin 3 (mCh-Gal3) were treated with 60 μM chloroquine for 30 min and analyzed by immunofluorescence microscopy for Rabaptin5, transferrin receptor (TfR), and mCherry-galectin 3. Arrowheads point out swollen Rabaptin5-positive endosomes. Scale bar, 10 μm.

B Cells from experiments as in panel A were quantified for costaining of Rabaptin5-positive rings with transferrin receptor and galectin 3 (mean ± SD of three independent experiments counting > 50 rings each).

C HEK^{+Rbpt5} cells were treated without (–) or with 60 μM chloroquine (+CQ) or 1 mM LLOMe (+LLOMe) for 30 min and analyzed by immunofluorescence microscopy for Rabaptin5 and ALIX. Arrowheads point out swollen Rabaptin5-positive endosomes. Scale bar, 10 μm.

D HeLa cells stably expressing CHMP4B-GFP were treated as in panel C and analyzed for Rabaptin5, CHMP4B-GFP, and ALIX. Scale bar, 10 μm.

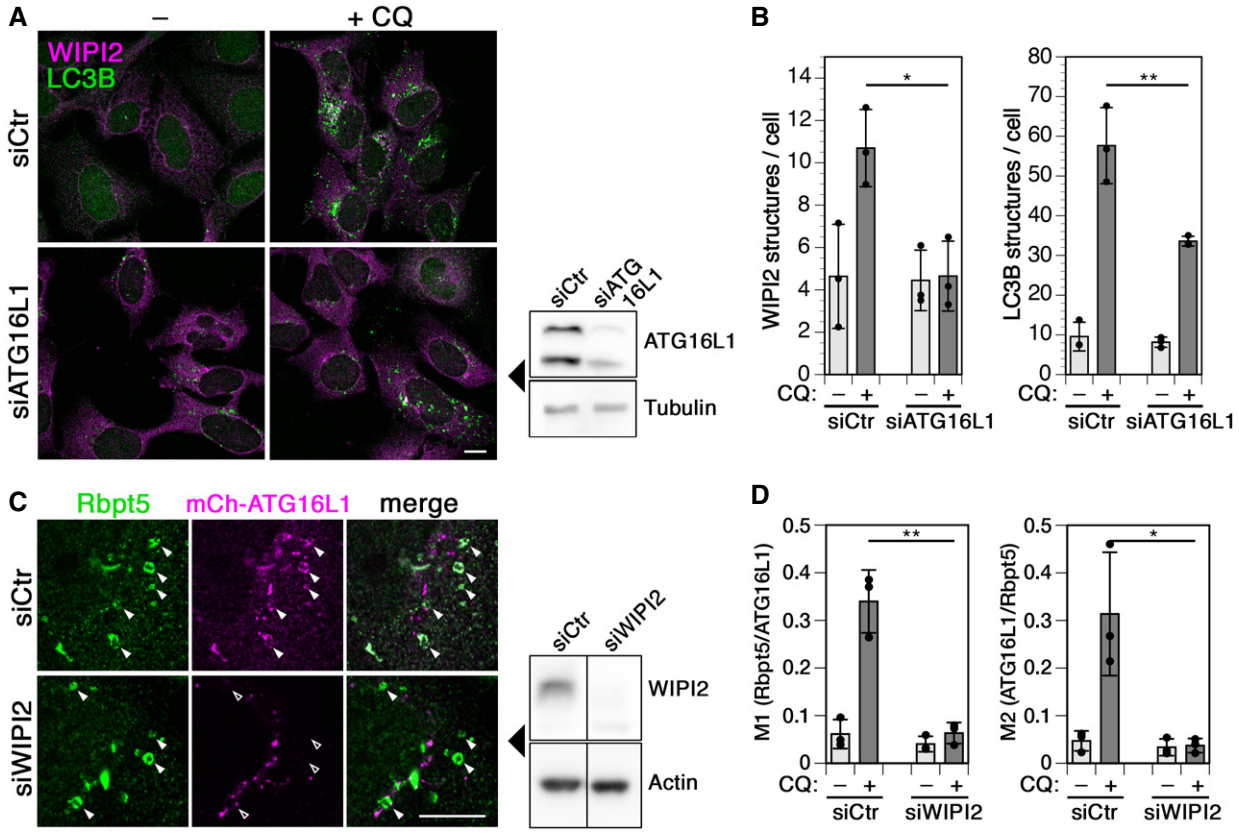

Figure EV3. Interdependence of WIPI2 and ATG16L1 recruitment to chloroquine-damaged endosomes.

A, B Cells were transfected with control siRNA (siCtr) or siRNA silencing ATG16L1, treated without (–) or with 60 μM chloroquine (+CQ) for 150 min, fixed, and stained for WIPI2 and LC3B (A). Scale bar, 10 μm. Efficiency of ATG16L1 knockdown was assayed by immunoblotting on the right. WIPI2 of LC3B puncta per cell was quantified for each condition (mean ± SD of three independent experiments; two-tailed Student's *t*-test: **P* < 0.05, ***P* < 0.01).

C HEK^{+Rbpt5} cells were transfected with nontargeting siRNA (siCtr) or siRNAs silencing WIPI2 (siWIPI2) for 72 h and with mCherry-ATG16L1 for 24 h. Cells were treated without or with 60 μM chloroquine (+CQ) for 30 min and stained for Rabaptin5 and mCherry-ATG16L1. Fluorescence micrographs of chloroquine-treated cells are shown (left panel). Scale bar, 10 μm. Arrowheads point out chloroquine-induced enlarged early endosomes. The efficiency of WIPI2 knockdown was assayed by immunoblotting using actin as a loading control (middle panel).

D Manders' colocalization coefficients were determined, M1 showing the fraction of Rabaptin5-positive structures also positive for mCherry-ATG16L1 and M2 showing the inverse. Mean ± SD of three independent experiments; ANOVA: **P* < 0.05, ***P* < 0.01.

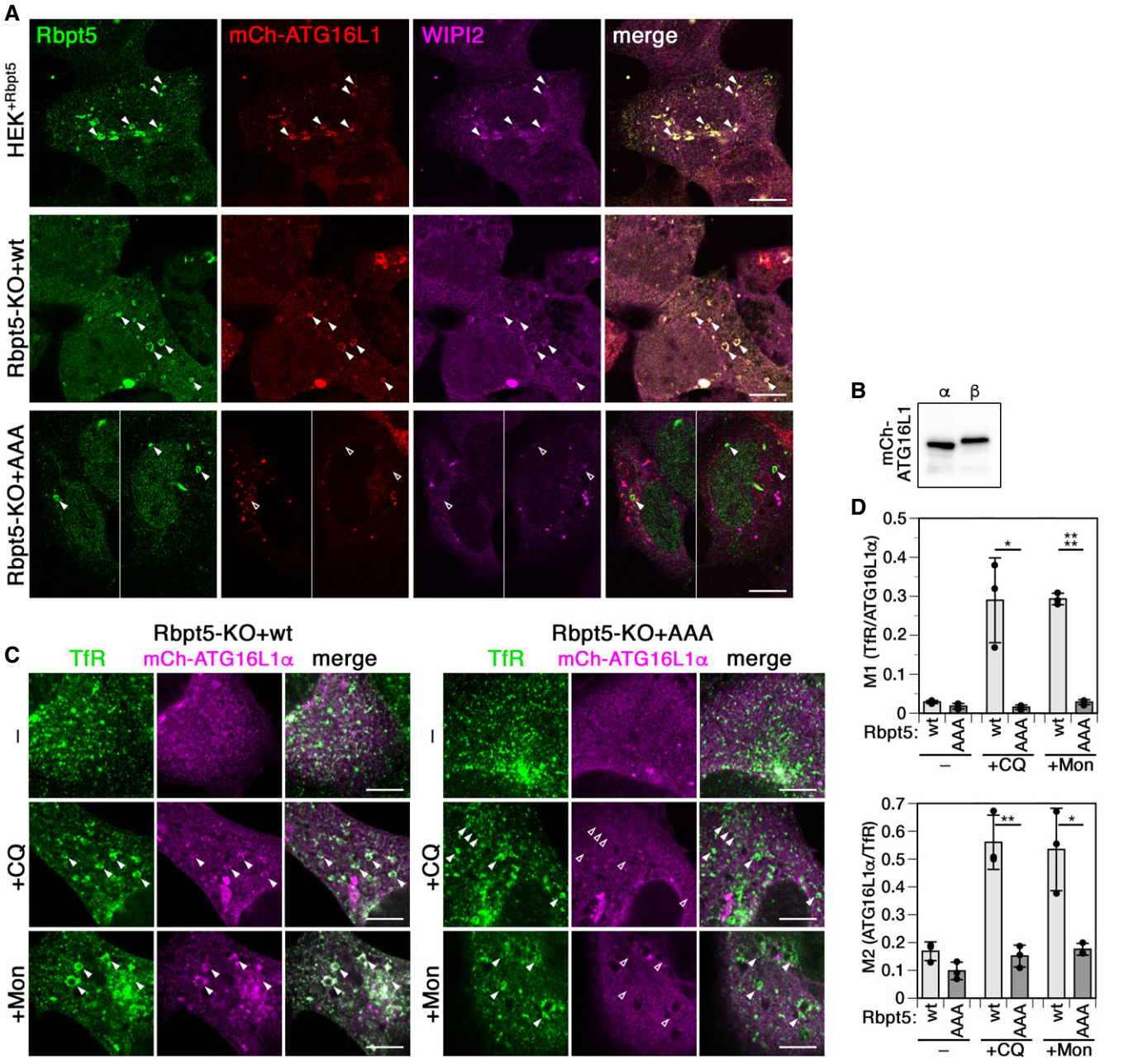

Figure EV4. Recruitment of full-length ATG16L1 and ATG16L1α to damaged endosomes depends on the interaction motif in Rabaptin5.

A HEK^{+Rbpt5} cells and Rabaptin5-knockout cells stably re-expressing wild-type (Rbpt5-KO+wt) or AAA mutant Rabaptin5 (Rbpt5-KO+AAA) were transfected with mCherry-ATG16L1, treated with 60 μM chloroquine (CQ) for 30 min, and analyzed by immunofluorescence microscopy for Rabaptin5, mCherry-ATG16L1, and WIPI2. Manders' colocalization coefficients determined from these experiments are shown in Fig 6F and G. Scale bar, 10 μm. Arrowheads point out enlarged Rabaptin5-positive endosomes (empty arrowheads when negative for the stained protein).

B HEK293A cells were transfected with the mCherry-tagged full-length b isoform of ATG16L1 or the a isoform lacking residues 266–284 and analyzed by immunoblot analysis.

C Rabaptin5-knockout cells stably re-expressing wild-type (Rbpt5-KO+wt) or AAA mutant Rabaptin5 (Rbpt5-KO+AAA) were transfected with mCherry-ATG16L1α, treated without (–) or with 60 μM chloroquine (+CQ) or 100 μM monensin (+Mon) for 30 min, and analyzed by immunofluorescence microscopy for the transferrin receptor (TfR) and mCherry-ATG16L1α. Arrowheads point out chloroquine-induced enlarged early endosomes. Scale bar, 10 μm. Arrowheads point out enlarged Rabaptin5-positive endosomes (empty arrowheads when negative for the stained protein).

D From experiments as in panel C, Manders' colocalization coefficients were determined, M1 showing the fraction of transferrin receptor-positive structures also positive for mCherry-ATG16L1α and M2 showing the inverse (mean ± SD of three independent experiments; two-tailed Student's *t*-test: $*P < 0.05$, $**P < 0.01$, $****P < 0.0001$).

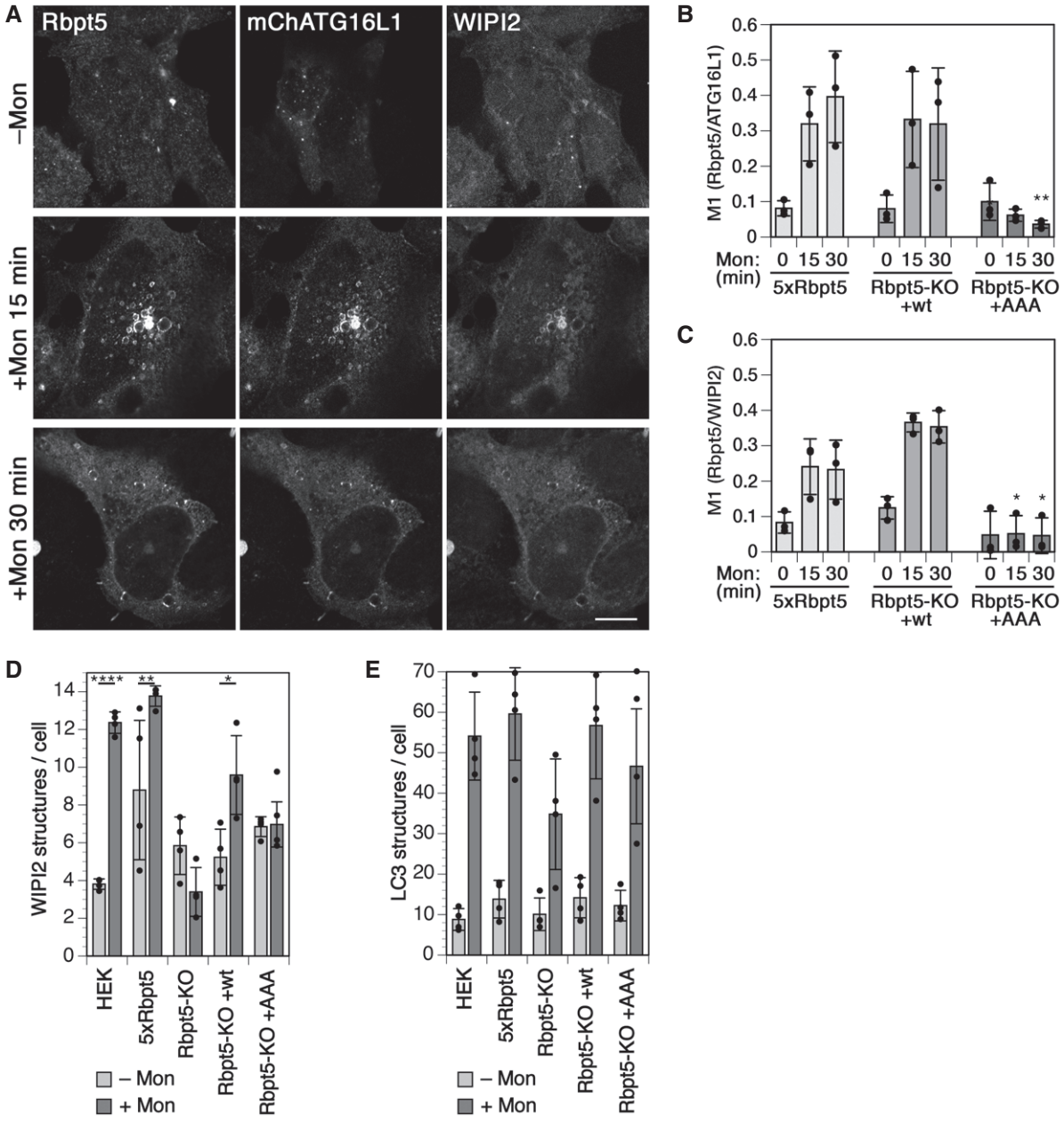

Figure EV5. Monensin induces endosomal autophagy dependent on Rabaptin5 and ATG16L1-binding just like chloroquine.

A HEK^{+Rbpt5} cells, 24 h after transfection with mCherry-ATG16L1, were treated with 100 μM monensin for 0, 15, and 30 min and stained for Rabaptin5, WIPI2, and mCherry-ATG16L1 to assess their colocalization on swollen early endosomes. Scale bar, 10 μm.

B, C Manders' colocalization coefficients were determined, showing the fraction of Rabaptin5-positive structures also positive for mCherry-ATG16L1 (B) or for WIPI2 (C) (mean ± SD of three independent experiments, quantifying ~40 cells for each sample; ANOVA for Rbpt5-KO+AAA versus HEK^{+Rbpt5} cells : *$P < 0.05$, **$P < 0.01$).

D, E Wild-type HEK293A cells, HEK^{+Rbpt5} cells, and Rabaptin5-knockout cells without (Rbpt5-KO) or with stable re-expression of wild-type (Rbpt5-KO+wt) or AAA mutant Rabaptin5 (Rbpt5-KO+AAA) were treated without (–Mon) or with 100 μM monensin for 150 min (+Mon), and analyzed by immunofluorescence microscopy for WIPI2 or LC3B. WIPI2 (D) of LC3B (E) puncta per cell were quantified for each condition (mean ± SD of four independent experiments; ANOVA: *$P < 0.05$, **$P < 0.01$, ****$P < 0.0001$).

